JAERI-M
7800

A POSITION-SENSITIVE START DETECTOR FOR TIME-OF-FLIGHT MEASUREMENT

August 1978

Hiroshi IKEZOE, Goro ISOYAMA* and Naomoto SHIKAZONO

日本原子力研究所
Japan Atomic Energy Research Institute

JAERI-M 7800

A Position-Sensitive Start Detector for Time-of-Flight Measurement

Hiroshi IKEZOE, Goro ISOYAMA* and Naomoto SHIKAZONO

Division of Physics, Tokai Research Establishment, JAERI

(Received July 18, 1978)

A position-sensitive start detector for a time-of-flight measurement is described. In this detector microchannel plates were used to obtain time and position signals simultaneously. A time resolution of 121 psec FWHM and a position resolution of 0.28 mm FWHM were obtained for α-particles from an ^{241}Am source.

Keywords: Start Detector, Resistive Plate, Microchannel Plates, Emission Angle, Time-of-Flight Measurement, Time Resolution, Position Resolution.

---

* Department of Physics, Tohoku University, Sendai, Japan.

飛行時間法のための位置検出可能な時間零検出器

日本原子力研究所東海研究所物理部
池添　博・磯山　悟郎*・鹿園　直基

（1978年7月18日受理）

飛行時間法に使われる位置検出可能な時間零検出器を製作した。この検出器では，マイクロチャンネルプレートを使用しており，位置及び時間が同時に検出可能である。^{241}Amからのα粒子を使って，時間分解能121 psec（FWHM），位置分解能0.28 mm（FWHM）が得られた。

*東北大学理学部

Contents

目　　次

1. Introduction

In order to measure masses of heavy-ion reaction products, the time-of-flight technique (TOF) is frequently used. A fast timing technique utilizing microchannel plates (MCP) has been extensively developed.[1,2] Secondary electrons produced when the heavy-ion reaction products pass through a thin carbon foil are detected and amplified by the MCP. Fast timing signals from the MCP provide start signals for the TOF measurement. In addition to the fast timing, the MCP has an excellent position resolution.[3] By making the best of these properties of the MCP, a position-sensitive start detector with a fast timing is constructed.

The secondary electrons emitted from the thin carbon foil are focused onto the MCP in a uniform magnetic field and then amplified by the MCP without losing a position information. The timing and the position signals are simultaneously obtained from a resistive plate placed behind the MCP. From the position signals, one can determine the particle trajectory when this detector is placed in the entrance of a TOF spectrometer. Generally, a large solid angle gives a large flight time difference because of the different path lengths for particles starting with the different angles. Therefore the present position-sensitive start detector has the substantial advantage when it is applied to the TOF measurement in a high-resolution magnetic spectrometer with a large solid angle.

2. Experimental Device

A structure of the position-sensitive start detector is shown in Fig. 1. The experimental device is almost the same as one reported in ref. 1, except that the resistive plate is placed at an anode position of the MCP in order to measure positions on the thin carbon foil where reaction products pass through.

Alpha-particles (5.486 MeV) from an ^{241}Am source hit the thin carbon foil (about 10 $\mu g/cm^2$ thickness, 10 mm in diameter) which is perpendicular to incident α-particles. Secondary electrons emitted when the α-particles pass through the thin carbon foil are accelerated to approximately 1.2 keV by an acceleration grid of 99 % transmission. They are then transported 180° in a homogeneous magnetic field of 50 G. The 180° transport system

containing a quater-turn slit placed at the 90° position has the advantage of shielding the MCP from the background electrons and X-rays. An inhomogeneity of the magnetic field B causes flight-time differences of the secondary electrons, resulting in the deterioration of the time resolution. In the present detector, however, $\Delta B/B$ is less than 2 % in the whole region of a Faraday cage, and it turns out that the effect of the magnetic inhomogeneity is unimportant.

In front of the MCP a suppression grid is placed to reduce small satellite peaks appeared in the time-of-flight spectrum.[1] The satellite peaks, as reported in ref. 1, are due to tertiary electrons emitted from an insensitive surface of the MCP which the secondary electrons hit. They again hit the MCP after some time delays in the magnetic field. In order to reject the tertiary electrons, the suppression grid and the acceleration grid are electrically connected to the Faraday cage and their voltage is more negative than that of the contact surface of the MCP. Voltages of various electrodes are shown in Fig. 2.

The two MCP* (active area of 20 mm in diameter, 0.66 mm thickness (upper) and 0.70 mm thickness (lower)) are mounted in a chevron configuration with a gain of 10^7 at an applied voltage of 1 kV for each MCP.

For the purpose of the timing experiment, a 50 Ω coaxial cone anode[1] was used to collect current pulses from the MCP. For the purpose of getting the fast timing and position signals simultaneously, the cone anode was replaced by a resistive plate (20 mm length and 20 mm width), which is made of ruthenium oxide/glass resistive ink blends fired on a 1 mm thick alumina substrate. The back of the alumina substrate is attached to a copper plate. The resistive plate is electrically equivalent to an RC transmission line. Total resistance R and total capacitance C of the line are determined to be 150 kΩ and about 35 pF, respectively, in order to minimize a position uncertainty due to the electronical noise.[4]

As shown in Fig. 3, position signals obtained from the both side of the line are amplified by the charge-sensitive preamplifiers. The position information is extracted by means of a risetime method developed by several authors.[5,6] The risetimes of both output pulses are proportional to positions where electrons from the MCP are incident upon the resistive plate, and they are converted to the zero-cross times of bipolar signals from the linear amplifiers. The difference between zero-cross times of

* Purchased from Hamamatsu TV CO., Ltd. Hamamatsu, Shizuoka, Japan.

the bipolar signals is converted to a pulse height by the time-to-amplitude converter (TAC) and analyzed by a multichannel analyzer.

Induced current impulses are obtained through the 50 Ω coaxial cable attached to the back of the alumina substrate. Their risetimes and pulse widths were observed to be exactly the same as those obtained by the 50 Ω cone anode. These fast timing signals are directly input to the constant fraction discriminator (CFD, ORTEC 473A) without any amplification because of their large amplitudes.

3. Experimental Results

3.1 Pulse height distribution of slow signal

Pulse height distributions of slow signals from the MCP are shown in Fig. 4. As shown in Fig. 2, the slow signals are extracted from a final electrode of the MCP through the charge-sensitive preamplifier. The pulse height spectra are recorded with a coincidence requirement from a surface barrier detector in order to reject random pulses due to a dark current of the MCP itself. The pulse height distribution has a broad bump with a long tail. This characteristic shape is ascribed to a statistical process in the electron multiplification of the MCP and to a number uncertainty of the secondary electrons produced when α-particles pass through the thin carbon foil. The number of the secondary electrons depends on the atomic number Z of the incoming particles and its mean is probably less than 10 for the α-particles.[7] Thereby its statistical fluctuation becomes large for light particles such as α-particles.

Figure 4 also shows a dependence of the spectrum shape on a vacuum pressure. A component of small pulse heights under the broad bump appears in a higher pressure of 1×10^{-5} Torr. This component probably arises from some contaminations on the inside surface of each channel of the MCP. It has been reported that a deposition of a diffusion-pump oil on the multipliers is responsible for a decrease of the gain of the MCP.[8] Actually this component somewhat decreased after the MCP was washed by a supersonic cleaner.

In order to examine the dependences of the pulse height distribution and of an emission power of the secondary electrons on the materials of thin foils, the 10 μg/cm^2 KCl and the 10 μg/cm^2 NaCl evapolated on the carbon backing of the 10 μg/cm^2 thickness were tried. Almost the same spectra as shown in Fig. 4 were obtained for these foils. The secondary

electrons increased in number twice as large as in the case of the thin carbon foil of the 10 $\mu g/cm^2$ thickness. This result suggests that the emission power of the secondary electrons simply depends on the total energy loss of the incoming particles in the thin foils.

3.2 Emission angle of the secondary electrons

In the present device a flight time T of the secondary electrons from the thin carbon foil to the MCP is 3.4 nsec. Therefore in order to obtain the fast timing the flight-time different ΔT has to be minimized at least less than a few percentage of the total flight time. A path length L along the secondary electron orbital depends on the emission angle θ. The path-difference ΔL between a center orbital (θ=0) and the other orbital of the emission angle $\theta(\neq 0)$ is written as $\Delta L = 2L\theta/\pi$. The ΔT, therefore, is expressed as follows; $\Delta T = 2\Delta LT/L = 4\rho\theta/\sqrt{2V/m}$, where V,m and ρ are an acceleration voltage, an electron mass and an orbital radius, respectively. The angular distribution of the secondary electrons also affects a position resolution. Here we adopt a coordinate system shown in Fig. 1. By a simple calculation, x and y position displacements Δx, Δy from the center orbital at the MCP position are written as $\Delta x = \rho\theta^2$, $\Delta y = \pi\rho\theta$. The effective angle θ_e can be obtained from the measurement of the y-position dispersion Δy directly. To measure the Δy, the resistive plate was set parallel to the y-axis and a single-hole slit (2 mm in diameter) was placed just before the thin carbon foil to collimate the incident α-particles. A position spectrum of the secondary electrons emitted in the forward direction is shown in Fig. 5a. The measured $2\Delta y$ is 5.4 mm FWHM and the effective angle θ_e is calculated as 2.0°. The ΔT is then estimated to be 152 psec for the secondary electrons emitted in the forward direction. The ΔT can be reduced by making use of the secondary electrons emitted in the backward direction. Figure 5b shows the position spectrum of these secondary electrons. The $2\Delta y$ of the position distribution was 3.6 mm FWHM for these secondary electrons and the smaller flight-time difference ΔT = 90 psec was estimated. The number of the secondary electrons emitted backward was, however, approximately 0.5 times smaller than that emitted forward. This problem can be get over by using thicker carbon foil than the present one, and there is no problem for the heavy ions incident, becasue they produce many secondary electrons.[7)]

An acceleration of the secondary electrons in a stronger electric

field than 1.2 kV will be a direct improvement to reduce the effective angle. This effect will be discussed in Sec. 4.

3.3 Time resolution

A time resolution was measured by means of the TOF technique by arranging the two same devices as shown in Fig. 6. In order to get a good time resolution an electronical walk of the CFD had to be minimized. A voltage dynamic range of the input fast signals to the CFD was larger than 1:10 because of the characteristic pulse height distribution. The walk was minimized by optimizing a delay time and a fraction rate for the constant fraction timing. Using a pulse generator, the overall time resolution of the electronics was obtained to be 30 psec for the dynamic range of 1:1. Since the path lengths of the electron orbitals depend on the emission angles, the timing test was done with changing an aperture size of the quater-turn slit. The time resolutions obtained were 272 psec, 215 psec and 189 psec FWHM for aperture sizes of 3 mm, 1 mm and 0.6 mm, respectively. A transmission efficiency of the secondary electrons for the aperture size of 0.6 mm is about half of that for the aperture size of 3 mm. A maximum dispersion of the secondary electrons at the quater-turn slit is estimated to be 1.6 mm from the measured effective angle θ_e. The observed transmission effeciencies are consistent with those expected from the measured effective angle. Figure 7 shows the TOF spectra obtained with the aperture size of 0.6 mm. From the measured value of 272 psec FWHM for the aperture size of 3 mm and the value of 152 psec estimated for the flight-time difference, the time resolution due to the electronics was estimated to be 118 psec.

The timing measurement utilizing the secondary electrons emitted in the backward direction was also done and a better time resolution of 171 psec FWHM was obtained for the 0.6 mm aperture size. From Fig. 7b one can obtain an intrinsic time resolution of single MCP arrangement by dividing the observed width by $\sqrt{2}$. This gives 121 psec time resoltuion for the backward emission of the secondary electrons. The results for the timing experiment are summerized in Table 1. The flight-time differences for each aperture sizes are calculated assuming the 118 psec time resolution of the electronics.

3.4 Position resolution

A measurement of the position resolution was carried out with the single MCP arrangement as shown in Fig. 3. At an exit of α-particles passed through the thin carbon foil the surface barrier detector was mounted and the resistive plate was placed along the x-axis. The result is shown in Fig. 8, where an image of a screen with two holes of 0.2 mm in diameter placed at the side of the thin carbon foil facing the ^{241}Am source is cleary displayed. From a measured width of 0.35 mm FWHM, an intrinsic position resolution was determined to be 0.28 mm FWHM.

4. Conclusion

The present device was developed as a position-sensitive start detector with a fast timing for the TOF technique and gave a good timing (121 psec) and a good position resolution (0.28 mm). In this device the emission angle of the secondary electrons plays an important role in its performance. The acceleration voltage used in the present device was 1.2 kV which was rather low. The higher voltage will give the smaller effective angle for the electrons emitted from the carbon foil. The more acceleration of the secondary electrons in a strong magnetic field (≈100G) has the advantage of a reduction of the flight time in addition to the reduction of the effective angle. By these improvements, more excellent performance should be expected.

References

1) A.M. Zebelman, W.G. Meyer, K. Halbach, A.M. Poskanzer, R.G. Sextro, G. Gabor and D.A. Landis, Nucl. Instr. and Meth. 141 (1977) 439.
2) J. Girard and M. Bolore, Nucl. Instr. and Meth. 140 (1977) 279.
3) W. Parkes, K.D. Evans and E. Mathieson, Nucl. Instr. and Meth. 121 (1974) 151.
4) E. Mathieson, Nucl. Instr. and Meth 97 (1971) 171.
5) R.B. Owen and M.L. Awcock, IEEE Trans. Nucl. Sci. NS-15 (1968) 290.
6) C.J. Borkowski and M.P. Kopp, Rev. Sci. Instr. 39 (1968) 1515.
7) H.-G. Clerc, H.J. Gehrhardt, L. Richter and K.H. Schmidt, Nucl. Instr. and Meth. 113 (1973) 325.
8) Ö. Nilsson, L. Hasselgren, K. Siegbahm, S. Berg. L.P. Andersson, P.A. Tove, Nucl. Instr. and Meth 84 (1970) 301.

Table 1 The results of the time-of-flight measurement

	Forward			Backward
Aperture size (mm)	3	1	0.6	0.6
Observed time resolution (psec)	272	215	189	171
Intrinsic time resolution (psec)	192	152	134	121
Flight-time difference (psec)	152	96	63	27

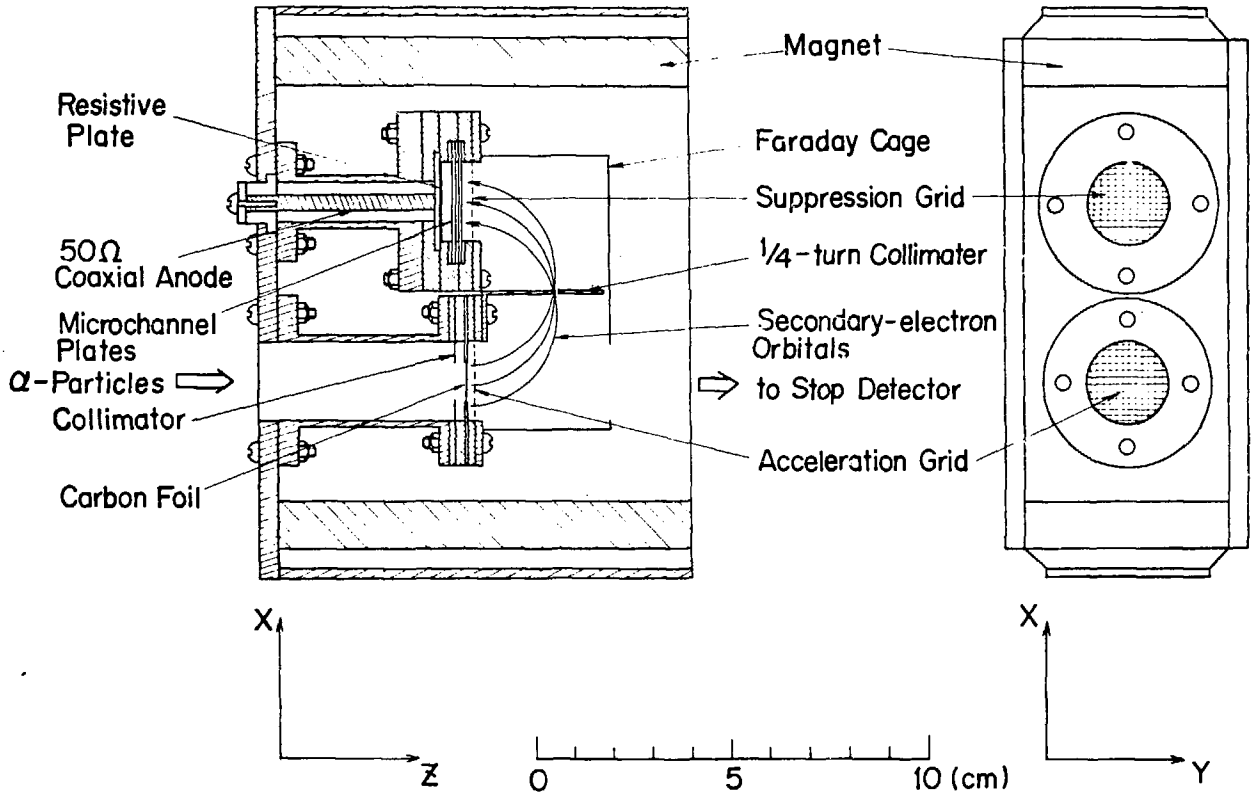

Fig. 1 The structure of the position-sensitive start detector.

JAERI-M 7800

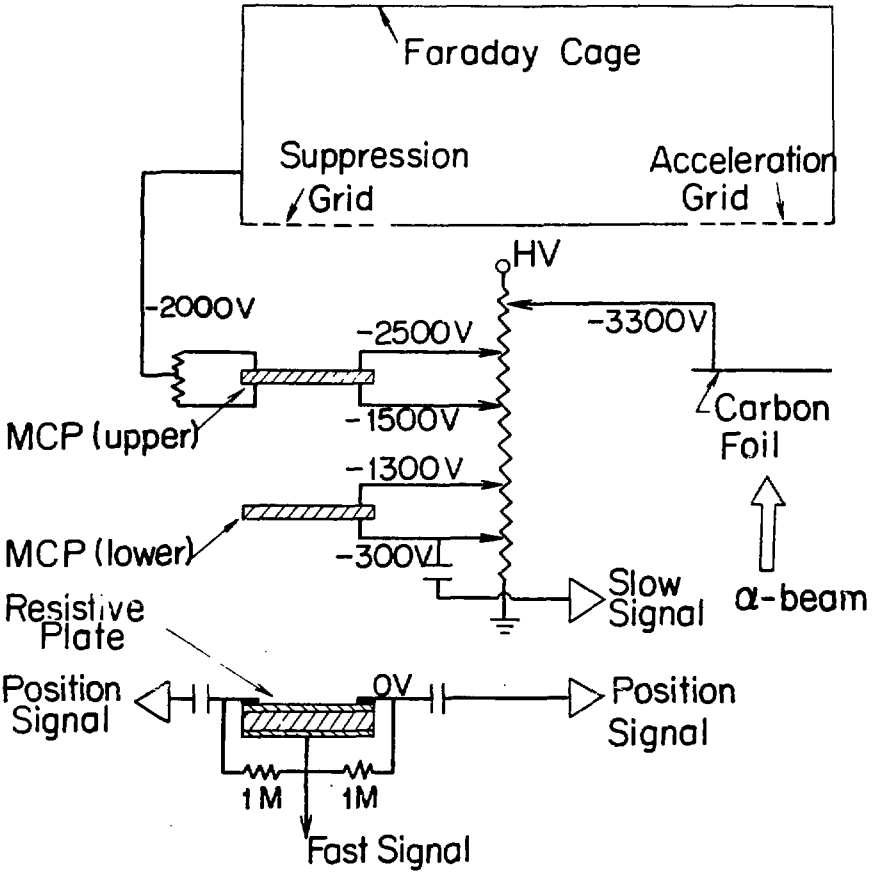

Fig. 2 Schematic diagram of voltage bias. A 1 MΩ resistor between the resistive plate and the ground is a leak resistor for a discharge of the RC line after receipt of position signals.

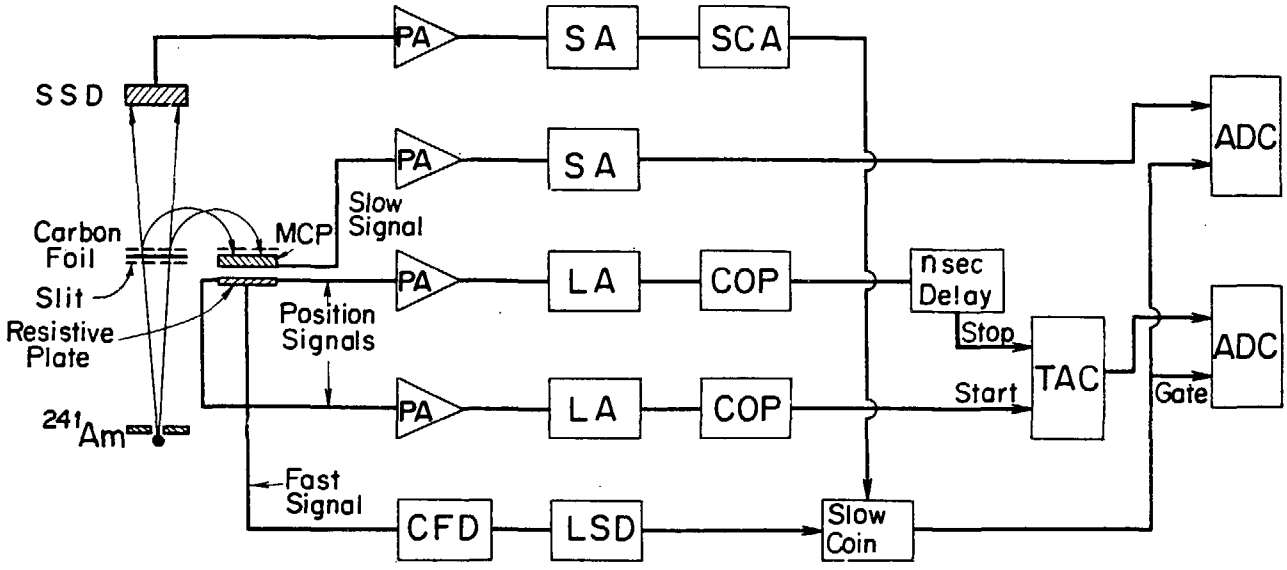

Fig. 3 An experimental arrangement and a block diagram of the electronics to obtain the position and the pulse height spectra. PA : charge-sensitive preamplifier.

SA : spectroscopy amplifier. SCA : single channel analyzer. CFD : constant fraction discriminator. LA : linear amplifier. COP : crossover pickoff. LSD : logic shaper and delay. TAC : time-to-amplitude converter. ADC : analog-to-digital converter. SSD : solid state detector.

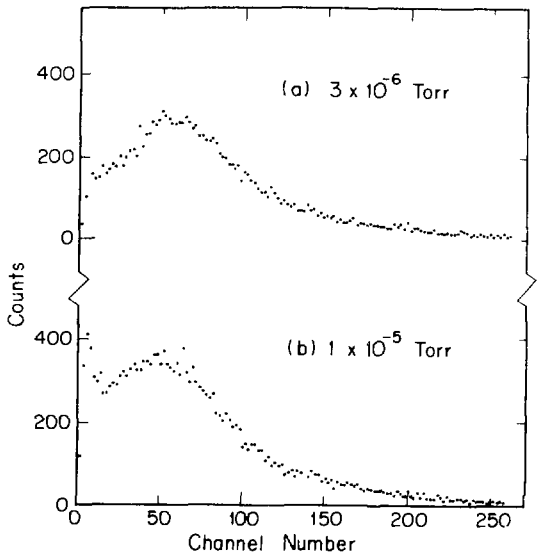

Fig. 4 The pulse height spectra of the MCP recorded with a coincidence requirement from the SSD, obtained at the pressure (a) of the 3×10^{-6} Torr and (b) of the 1×10^{-5} Torr.

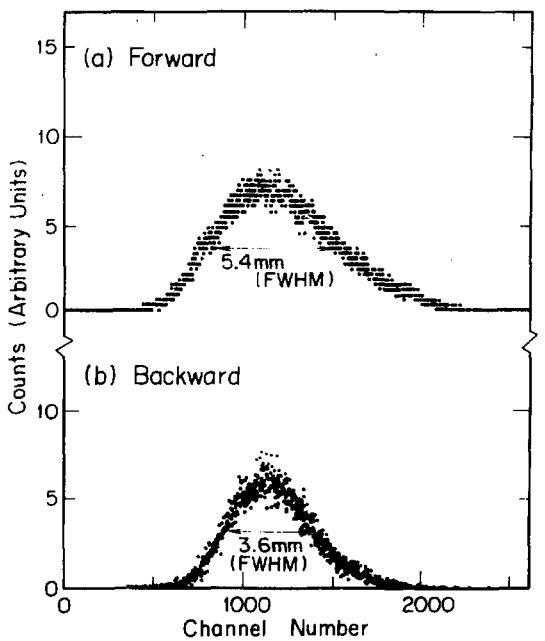

Fig. 5 The y-dispersion of the secondary electrons emitted (a) in the forward direction and (b) in the backward direction.

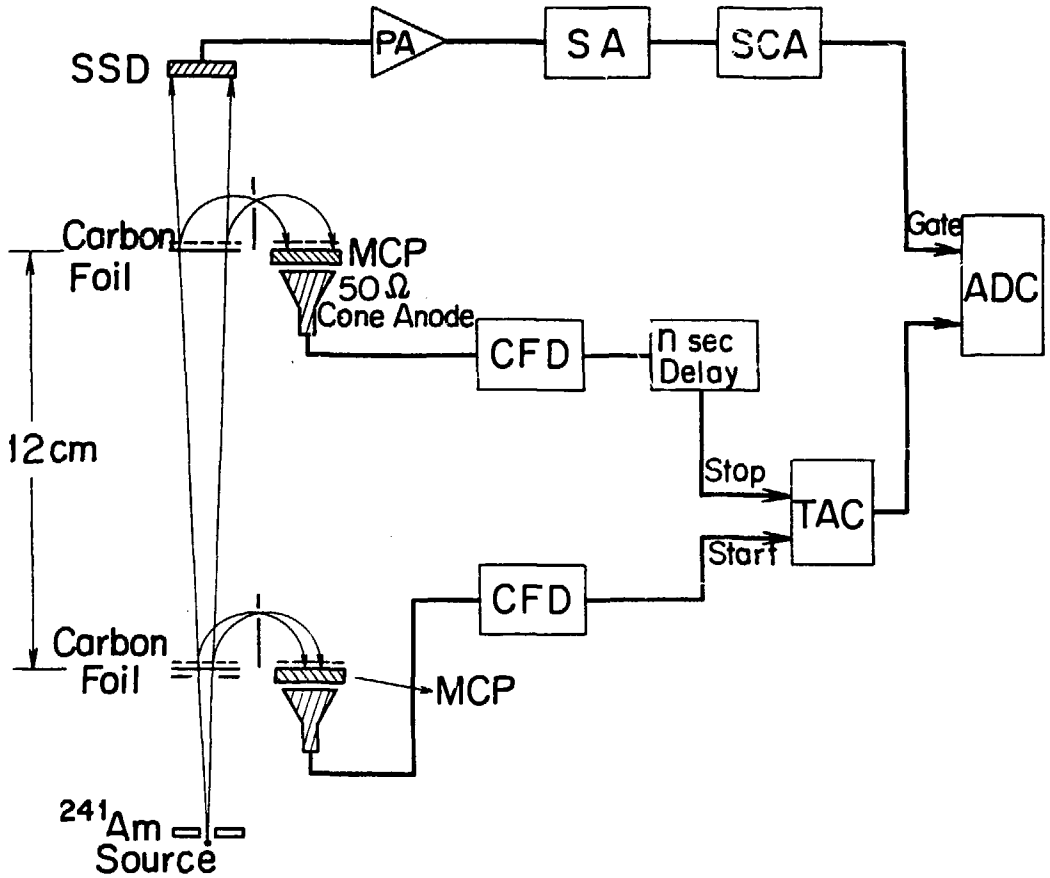

Fig. 6 A schematic arrangement and a block diagram of the electronics for the time-of-flight measurement.

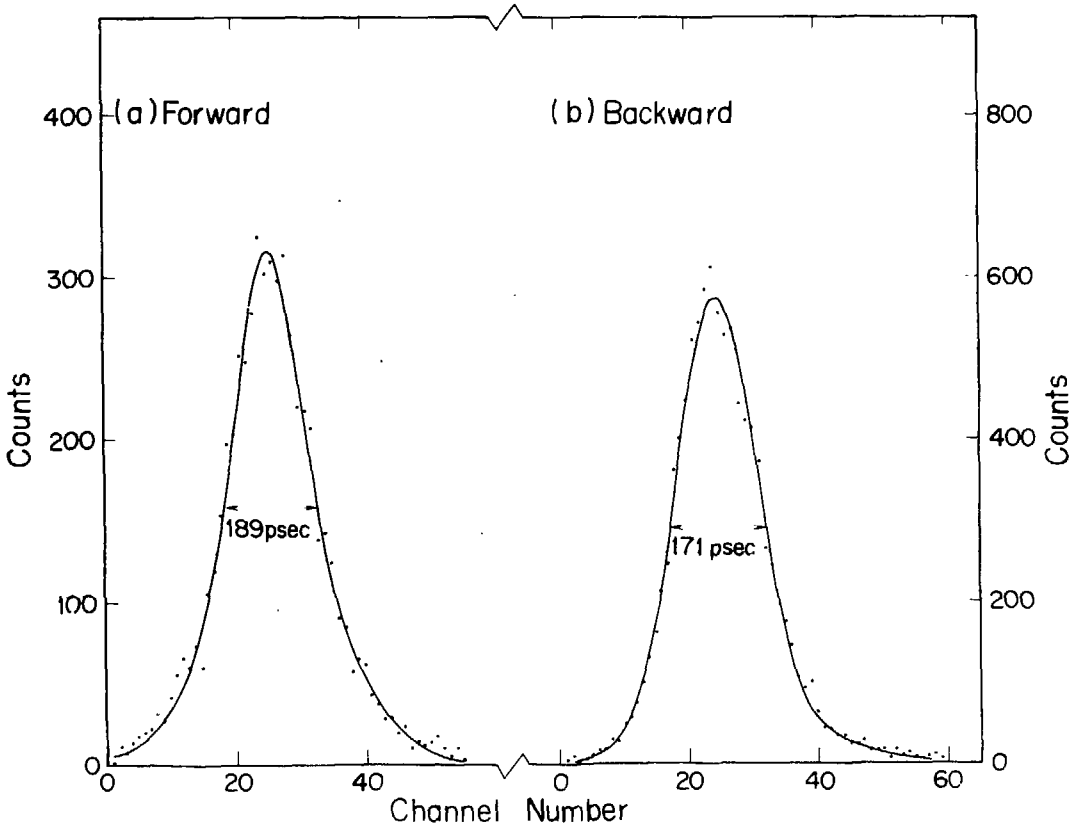

Fig. 7 Time-of-flight spectra (a) for the secondary electrons emitted in the forward direction and (b) for the backward emission of the electrons.

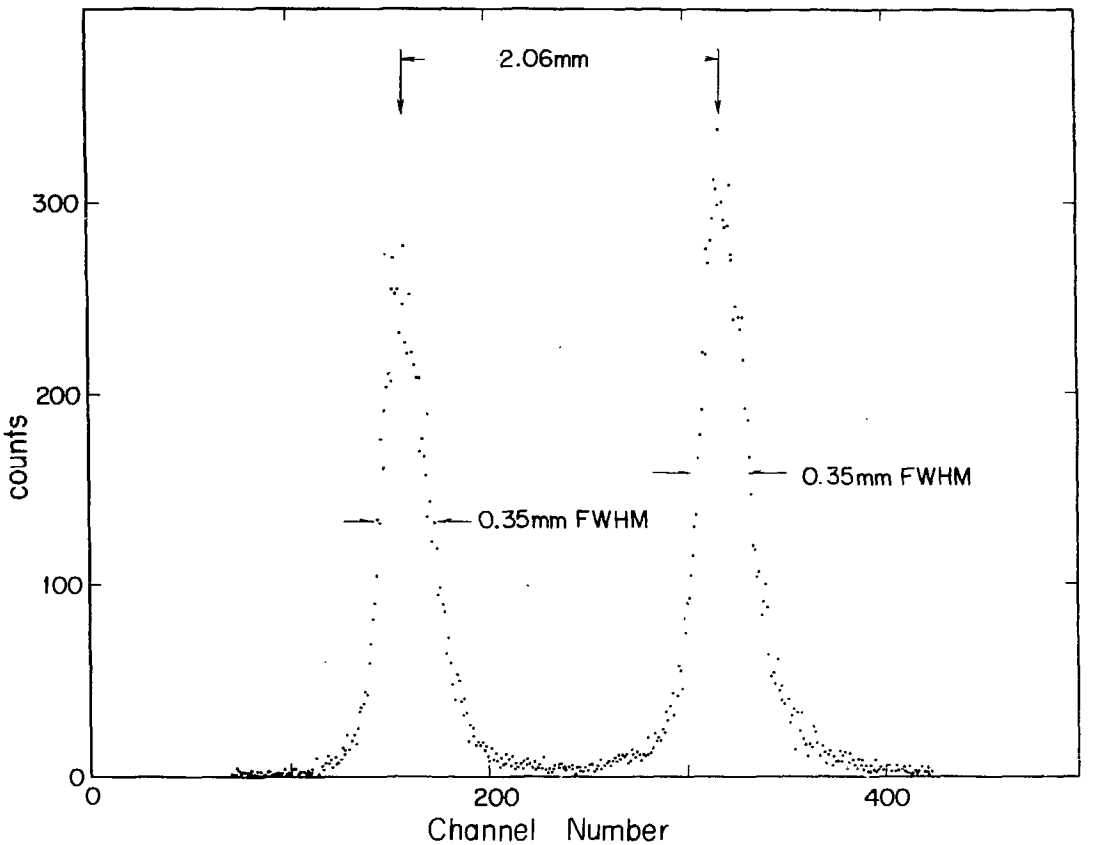

Fig. 8 The position spectrum for the collimated α-beams. The resistive plate was placed along the x-axis and a screen with two holes of 0.2 mm in diameter was set just before the carbon foil in order to collimate the incident α-particles. The secondary electrons emitted in the forward direction was detected.